Defence Science Journal, Vol. 75, No. 6, November 2025, pp. 779-787, DOI : 10.14429/dsj.20959

Study on the Energetic Characteristics of Gas Generating Compositions Based on Guanidinium Azotetrazolate

Nguyen Duy Tuan, Dam Quang Sang, Mai Van Thanh, and Hoang Trung Huu*

Faculty of Special Equipment, Le Quy Don Technical University, Ha Noi – 100 000, Viet Nam
**E-mail: hoanghuu@lqdtu.edu.vn*

ABSTRACT

Guanidinium Azotetrazolate (GAT) is a nitrogen-rich energetic compound with potential applications in environmentally friendly gas-generating pyrotechnics. This study investigates the combustion behavior of GAT-based formulations combined with various nitrate oxidizers (NaNO3, KNO3, Ba(NO3)2, and Sr(NO3)2) using phenol formaldehyde resin (PFR) as a binder fixed at 10 %. A compositional matrix was systematically designed, and key energetic properties were evaluated through both thermal analysis and combustion experiments. The Sr(NO3)2/GAT/PFR formulation at a 60/30/10 ratio exhibited the highest specific gas volume of 567.41 L.kg-1, accompanied by a relatively low heat of combustion of 779.95 kcal.kg-1. The KNO3/GAT/PFR system at a 70/20/10 ratio demonstrated a maximum burning rate of 4.48 mm.s-1, with a heat of combustion of 741.97 kcal.kg-1 and a specific gas volume of 421.81 L.kg-1. All tested compositions demonstrate low sensitivity to impact, friction, and thermal stimuli, indicating safe handling characteristics. These results highlight the potential of GAT-based formulations with PFR for use in efficient and safe gas-generating systems.

Keywords: GAT; Pyrotechnic; Gas generator; Combustion characteristic

NOMENCLATURE

GAT	: Guanidinium azotetrazolate
$NaNO_3$	: Sodium nitrate
KNO_3	: Potassium nitrate
$Ba(NO_3)_2$	: Barium nitrate
$Sr(NO_3)_2$	: Strontium nitrate
PFR	: Phenol-formaldehyde resin
NTO	: 3-nitro-2,4,5-triazole
NIGU	: Nitroguanidine
AP	: Ammonium perchlorate
W-Re	: Tungsten-Rhenium
DSC	: Differential scanning calorimetry
TG/DTA	:Thermogravimetry/differential thermal analysis
L, mm	: The length of samples
t, s	: The burning time of samples
u, mm.s^{-1}	: The linear burning rate
ΔP, mBar	:The pressure difference before and after combustion
T_c, K	: The chamber temperature
V_b, ml	: The bomb volume (334 ml)
m, g	: The mass of samples
W, L.kg^{-1}	: The specific volume of gaseous products
Q, kcal.kg^{-1}	: The heat of combustion
Ω, %	: The oxygen balance

Received : 15 April 2025, Revised : 08 July 2025
Accepted : 08 August 2025, Online published : 06 November 2025

1. INTRODUCTION

Solid gas-generating compositions play a crucial role in various applications, including pyrotechnic devices, rocket propellants, automotive airbag systems, and fire suppression technologies in both military and civilian sectors[1-6]. One of the primary advantages of solid gas generators is their remarkable efficiency; these systems are capable of producing substantial volumes of gas within a compact space. This adaptability allows their integration into a wide range of devices, while their rapid activation enables the generation of high gas pressures within short time-frames[7]. Furthermore, the manufacturing processes associated with such systems are relatively straightforward, facilitating large-scale production and thereby reducing overall costs. Additionally, their simple storage and transport requirements enhance their practicality for diverse operational needs. However, conventional gas-generating formulations, widely used in military and aerospace applications, present significant drawbacks. Their reliance on traditional components such as nitrocellulose and sodium azide results in the release of high levels of carbon monoxide and other toxic byproducts, primarily due to their inherent chemical and thermodynamic instabilities[8-10]. To address these challenges, modern gas-generating systems have been designed to produce high nitrogen (N_2) yields while minimising such adverse effects[8,11].

Recent research has therefore focused on "nitrogen-rich, carbon-poor" organic compounds as alternative gas-generating materials. These compounds offer several advantages over

traditional formulations, including high nitrogen content, low carbon content, high enthalpy of formation, high density, and reduced toxicity[12-15]. Notably, their nitrogen content can reach up to 80 %. For example, 3-nitro-2,4,5-triazole (NTO, 43 % N), nitroguanidine (NIGU, 53.9 % N), and GAT (78.8 % N) have been shown to generate substantial gas volumes per unit mass under specific conditions, making them promising candidates for environmentally friendly gas generation[16-18].

GAT is a high-nitrogen energetic material with significant potential for use in gas-generating systems and rocket propulsion[19-23]. Its unique properties enable the development of environmentally friendly smoke-generating materials, which are increasingly favoured across various applications. Recent studies have investigated the potential of combining GAT with oxidizers such as strontium nitrate to develop aerosol gas-generating formulations with effective fire-extinguishing capabilities[8-9]. When GAT is mixed with copper(II) nitrate trihydrate ($Cu(NO_3)_2 \cdot 3Cu(OH)$), the resulting formulation produces a specific volume of gaseous products of approximately 500 $L.kg^{-1}$, making it a preferred choice for automotive airbag applications due to its ability to generate completely non-toxic combustion products, ensuring user safety[24-26]. Additionally, a pyrotechnic composition comprising GAT and AP has been employed as a propellant in compact gas-generating devices designed for aerospace and missile applications; this formulation exhibits high-pressure generation capability while maintaining a relatively low combustion temperature of approximately 1400°C[27-28].

The investigation of GAT in combination with various oxidizers remains a developing area of research. A recent study[29] provided insights into the pyrotechnic properties of GAT-based mixtures with oxidizing salts such as lithium nitrate ($LiNO_3$), potassium nitrate (KNO_3), strontium nitrate ($Sr(NO_3)_2$), sodium nitrate ($NaNO_3$), and magnesium nitrate ($Mg(NO_3)_2$), formulated without the use of binders or resins. These binder-free gas-generating formulations displayed good thermal stability below 200 °C, fast combustion rates, and significant gas production. Among them, the GAT/KNO_3 composition was identified as the most promising due to its low moisture content, good powder fluidity, low friction sensitivity, excellent vacuum stability, and a high specific volume of gaseous products of 548.1 $L.kg^{-1}$. However, the omission of binders represents a limitation, as their presence in pyrotechnic formulations plays a critical role in shaping combustion behavior and influencing manufacturing processes.

Building on these findings, the present study investigates GAT-based pyrotechnic compositions containing $NaNO_3$, KNO_3, $Ba(NO_3)_2$, and $Sr(NO_3)_2$, with PFR incorporated as a binder at a fixed content of 10 wt %. A systematic compositional matrix was established to study the effects of oxidiser type and fuel ratio on combustion behaviour. Key parameters, including thermal decomposition, burning rate, heat of combustion, flame temperature, and specific gas volume, were measured experimentally, and sensitivity to impact, friction, and thermal stimuli was also evaluated. Additionally, computational simulations using the COMBUS software[30-31] were performed to compare theoretical predictions with experimental results.

2. METHODOLOGY

2.1 Chemical

GAT was synthesized and purified according to the procedure described in reference[30]. The final product exhibits a particle size range of 63-300 µm. Nitrate salts, including sodium nitrate ($NaNO_3$), potassium nitrate (KNO_3), barium nitrate ($Ba(NO_3)_2$), and strontium nitrate ($Sr(NO_3)_2$), were purchased from Xilong Co. Ltd., China, each with a particle size of ≤ 300 µm and a purity of ≥ 99 %. Acetone ($(CH_3)_2CO$) was of analytical reagent (AR) grade with a purity of 99.5 %, also obtained from Xilong Co. Ltd., China. Phenol formaldehyde resin (PFR, Idytol SF-0112) was supplied from the Russian Federation and conformed to GOST 18694-2017. It has a drop point of 117 °C, a free phenol content of 2.3 %, and was ground to a particle size of ≤ 100 µm before use. All chemicals were used as received, without any further purification.

2.2 Method

Caution: The substances and compounds investigated in this study possess high energetic and explosive potential. Therefore, strict safety precautions, including the use of gloves and protective eyewear, must be observed during handling.

2.2.1 Preparation of Samples

GAT was first dried in a hot water circulated oven for 4 hrs to remove moisture, then sieved through a 50-mesh screen to ensure uniform particle size. The oxidizer was ground, dried at 100 °C for 2 hrs, and likewise sieved through a 50-mesh screen. Both components were then blended and passed through the same sieve to achieve thorough mixing. Separately, PFR was dissolved in acetone to prepare the binder solution, which was subsequently mixed with the GAT–oxidizer blend for uniform dispersion. The resulting mixture was granulated by passing through a 30-mesh screen to obtain granules with the desired size and morphology. By using the above procedure twenty pyrotechnic compositions were prepared by changing the percentage of different oxidizers and GAT, keeping the percentage of PFR constant as per Table 1.

Following granulation, the pyrotechnic granules underwent a pre-drying stage lasting approximately 1 hour to facilitate partial evaporation of the PFR. They were then oven-dried at 60 °C for an additional 4 hrs to achieve complete drying. After drying, the granules were allowed to cool naturally to ambient temperature before being carefully stored in a desiccator to maintain stability and quality.

2.2.2 Measurements

Pyrotechnic samples were pressed into 6 mm × 25 mm acrylic cylinders at 1.5 $g.cm^{-3}$ using a hydraulic press. The burning rate was determined by measuring the time the burning surface travelled between two measuring heads placed a certain distance apart (L in mm). The burning time (t in sec.) was measured using a high-speed camera Handycam FDR-AXP55 (Sony, Japan). The linear burning rate u (in $mm.s^{-1}$) of the pyrotechnic samples was then calculated using the Eqn. (1):

$$u = \frac{L}{t} \tag{1}$$

Combustion temperature was recorded using a 50 µm W-Re thermocouple placed inside a half-cylinder acrylic tube (6 mm × 25 mm) with a trapezoidal top section. The sample was compressed to target density over the thermocouple, and the temperature signal was digitized and processed via a converter.

Combustion heat was measured using a Parr-6200 calorimeter (USA) with 1.5 g samples under a 80 mBar vacuum. The pressure was recorded by a Lutron-9017 manometer, with the bomb temperature maintained at ambient conditions. The specific volume of gaseous products was calculated using Eqn. (2):

$$W = \frac{273}{T_c} \cdot \frac{\Delta P \cdot V_b}{1000m} \quad (2)$$

Differential scanning calorimetry (DSC) analysis was performed on a Labsys DSC 131 (Setaram) at a heating rate of 10 °C.min^{-1} in an argon atmosphere. Thermogravimetric/differential thermal analysis (TG/DTA) of GAT was conducted using a DTG-60H (Shimadzu) with ~5 mg samples in aluminum crucibles.

Friction sensitivity was tested per STANAG 4487[31] using a BAM Friction Tester (Germany). Impact sensitivity followed GOST 4545-88[32] using Hammer K-44-II (Russia Federation). Ignition temperature was measured with a DT-400 device on 0.2 g dried, ground samples in test tubes, heated at 10 °C.min^{-1} until deflagration.

2.2.3 Thermo-Chemical Computations

The gas-generating pyrotechnic compositions were formulated with GAT as the primary gas-generating agent, while nitrate salts served as oxidizers due to their availability and ease of processing. PFR was employed as the binder because of its excellent combustion properties and relatively high thermal stability. Low PFR content adversely affects the mechanical and combustion properties, whereas excessive amounts diminish pyrotechnic performance and increase CO and CO_2 emissions. Consequently, the PFR content was fixed at 10 wt.% to ensure optimal pellet formation and mechanical integrity. The formulated compositions are summarized in Table 1. Their combustion parameters under isochoric conditions (0.222 m^3.kg^{-1}, 298 K) were calculated using the COMBUS software. The calculated specific volume of gaseous products and heat of combustion are also presented in Table 1.

Notably, the $NaNO_3$-based system exhibits the highest theoretical heat of combustion at a 75/15/10 ratio, unlike systems containing KNO_3, $Sr(NO_3)_2$, or $Ba(NO_3)_2$, which peak at 80/10/10. This phenomenon can be attributed to the oxygen balance (Ω) of the mixtures. At 75/15/10, the $NaNO_3$ system achieves an oxygen balance of -0.5%, the closest to zero among all tested compositions in that system. In contrast, for the other oxidizers, the oxygen balance approaches zero at 80/10/10.

The combustion of GAT/PFR-based pyrotechnics with various oxidizers produces gaseous products such as N_2, H_2, CO, and CO_2, along with solid residues of metal carbonates (Na_2CO_3, K_2CO_3, $BaCO_3$, $SrCO_3$). Fuel-rich mixtures (60/30/10) tend to yield more H_2 and CO due to reductive reactions, while oxidizer-rich compositions (80/10/10) favor complete combustion and solid carbonate formation.

The specific volume of gaseous products is a critical parameter, as an effective gas-generating pyrotechnic composition should produce a large specific volume upon combustion. The heat of combustion is another key factor influencing performance. Based on thermochemical calculations, the formulation $Ba(NO_3)_2$/GAT/PFR was identified as the most promising candidate. This composition not only demonstrates a high specific gas volume and favorable heat of combustion but also generates environmentally friendly combustion products.

3. RESULTS AND DISCUSSION

3.1 Characteristics of Pyrotechnic Samples

The microscopic structure of the pyrotechnic particles with an oxidizer/GAT/PFR ratio of 70/20/10 is shown in Fig. 1. The microstructure of the samples appears largely

Table 1. Calculation of pyrotechnic composition (Oxidizer/GAT/PFR) characteristics using COMBUS software

Composition, %	$NaNO_3$			KNO_3			$Ba(NO_3)_2$			$Sr(NO_3)_2$		
	Ω	*Q*	*W*	Ω	*Q*	*W*	Ω	*Q*	*W*	Ω	*Q*	*W*
80/10/10	5.8	852	281	-0.2	836	241	-7.4	634	276	-1.6	856	246
75/15/10	-0.5	1001	289	-6.1	756	318	-12.8	567	363	-7.4	775	326
70/20/10	-6.8	905	371	-12	675	407	-18.3	498	455	-13.3	693	416
65/25/10	-13.1	808	464	-18	595	502	-23.8	430	550	-19.1	611	511
60/30/10	-19.4	711	562	-23.9	514	600	-29.2	389	616	-24.9	529	609

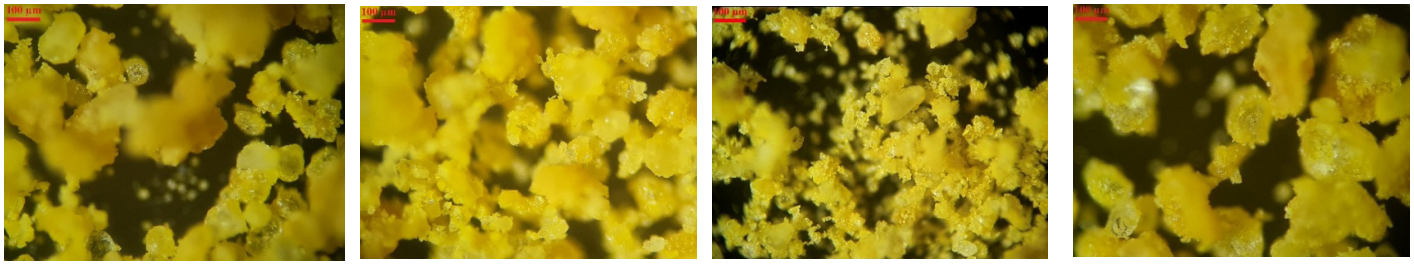

(a) (b) (c) (d)

Figure 1. Microscopic images of pyrotechnic samples at x300 magnification: (a) KNO3/GAT/PFR; (b) NaNO3/GAT/PFR; (c) Ba(NO3)2/GAT/PFR; and (d) Sr(NO3)2/GAT/PFR.

uniform. Image analysis using ImageJ software[33], reveals particle sizes ranging from 50 µm to 300 µm. The microscopic images show that, prior to compaction, the pyrotechnic particles exhibit irregular shapes but relatively uniform sizes. The characteristic yellow color indicates the predominant presence of GAT, which appears to be homogeneously distributed throughout the sample. The uniformity in both color and particle size suggests that the mixing process was effectively carried out, ensuring stability and compositional consistency before final compaction.

3.2 Thermal Decomposition

Thermogravimetric analysis (TG) and differential thermal analysis (DTA) were employed in this study to investigate the thermal decomposition behavior of GAT (Fig. 2), while differential scanning calorimetry (DSC) was used to characterize the thermal behavior of pyrotechnic samples composed of oxidizer/GAT/PFR at a ratio of 70/20/10 (Fig. 3). The DSC thermograms of all four compositions exhibit exothermic peaks at similar temperatures: 530.2 K (KNO_3), 531.2 K ($NaNO_3$), 537.1 K ($Ba(NO_3)_2$), and 535 K ($Sr(NO_3)_2$), which correspond to the decomposition of GAT. For reference, Fig. 2 shows that pure GAT decomposes at approximately 524.1 K.

In the pyrotechnic composition containing KNO_3, an endothermic peak at 414.4 K corresponds to the polymorphic phase transition of KNO_3 (from rhombohedral to trigonal)[34]. Additionally, an endothermic peak at 605.2 K indicates the melting of KNO_3, while an exothermic peak at 696.6 K corresponds to the thermal decomposition of the oxidizer salt. For the $NaNO_3$-based pyrotechnic composition, alongside the GAT decomposition peak, an endothermic peak at 582.3 K is attributed to the melting of $NaNO_3$, with its decomposition occurring at 687.1 K.

In contrast, the DSC thermograms of compositions containing $Ba(NO_3)_2$ and $Sr(NO_3)_2$ show no endothermic peaks aside from the exothermic peak linked to GAT decomposition. The decomposition temperatures of $Ba(NO_3)_2$ and $Sr(NO_3)_2$ exceed 773.15 K, indicating substantially higher thermal stability compared to GAT.

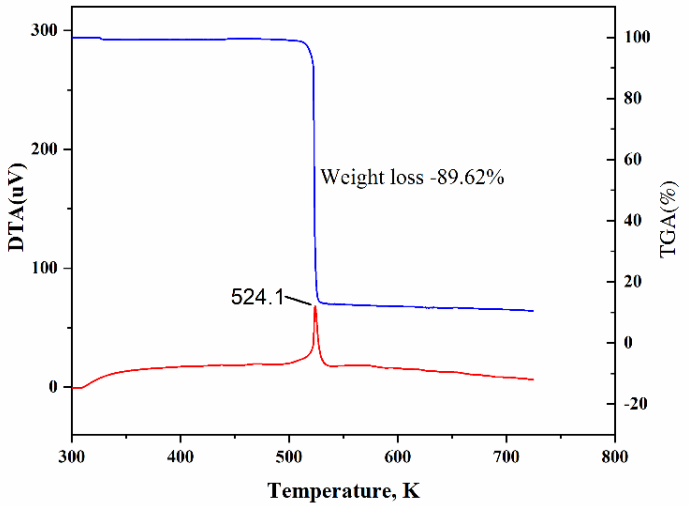

Figure 2. TG/DTA thermal analysis diagrams of GAT.

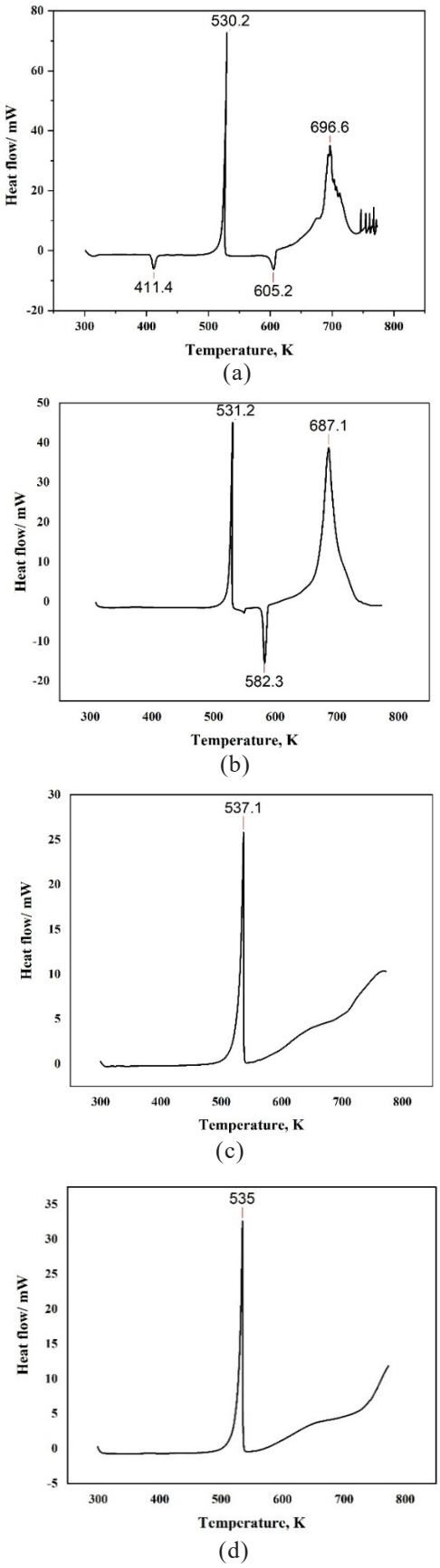

Figure 3. DSC thermal analysis diagrams of pyrotechnic samples with different oxidants: (a) KNO3/GAT/PFR; (b) NaNO3/GAT/PFR; (c) Ba(NO3)2/GAT/PFR; and (d) Sr(NO3)2/GAT/PFR.

3.3 Combustion Characteristics

The pyrotechnic compositions were compacted into tubes, and their linear burning rates were measured at atmospheric pressure. The results are presented in Fig. 4, which illustrates the relationship between the burning rate and the oxygen balance of the compositions. During combustion, potassium nitrate (KNO_3) and sodium nitrate ($NaNO_3$) produce characteristic yellow flames, while barium nitrate ($Ba(NO_3)_2$) emits a bright white flame, and strontium nitrate ($Sr(NO_3)_2$) generates a vivid red flame, as shown in Fig. 5.

In the $NaNO_3$/GAT/PFR and KNO_3/GAT/PFR systems, combustion fails or does not ignite when the oxygen balance is less than or equal to -19.4 % (at ratio 60/30/10) and -18.0 % (at ratio 65/25/10), respectively. This is attributed to insufficient oxygen supply from the decomposed previous layers to sustain combustion in the subsequent layers. In contrast, the $Ba(NO_3)_2$/GAT/PFR and $Sr(NO_3)_2$/GAT/PFR systems do not exhibit such combustion limits within the tested oxygen balance range. For the KNO_3/GAT/PFR system, the 85/5/10 composition (Ω=5.7 %) was prepared to obtain additional data on the burning rate.

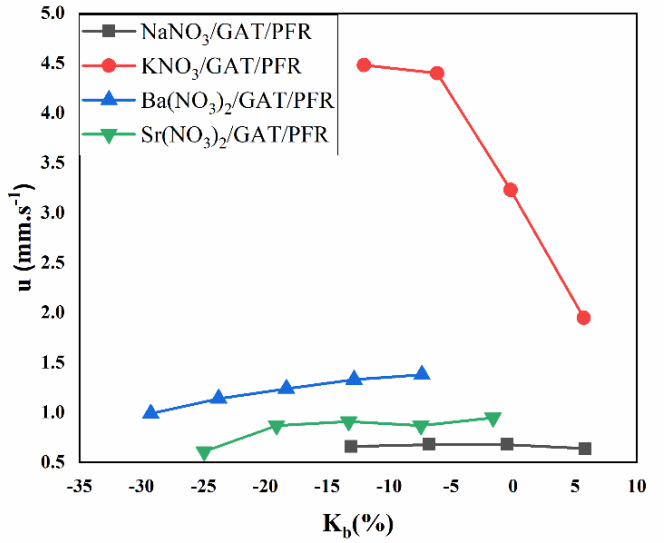

Figure 4. Effect of oxygen balance on the burning rate of pyrotechnic compositions.

The burning rates of the $NaNO_3$/GAT/PFR, $Ba(NO_3)_2$/GAT/PFR, and $Sr(NO_3)_2$/GAT/PFR systems exhibit minimal dependence on Ω, with values in the ranges of 0.64-0.68 $mm.s^{-1}$, 0.99-1.33 $mm.s^{-1}$, and 0.61-0.91 $mm.s^{-1}$, respectively. In contrast, the burning rate of the KNO_3/GAT/PFR system is significantly affected by Ω. Specifically, the burning rate decreases as Ω increases, reaching a maximum value of approximately 4.48 $mm.s^{-1}$ at a Ω of -12 %. When Ω rises to 5.72 % (at ratio 85/5/10), the burning rate drops to 1.95 $mm.s^{-1}$. This behavior is attributed to the excess oxygen present at higher Ω values, which reduces the proportion of fuel, such as GAT, in the mixture. Consequently, insufficient fuel is available to provide the energy necessary to sustain rapid oxidizer decomposition, leading to a decreased burning rate.

Combustion temperatures of GAT and pyrotechnic compositions with a 70/20/10 ratio were measured at ambient temperature and atmospheric pressure. The combustion temperature profiles are shown in Fig. 6. GAT exhibited the lowest combustion temperature (T_{max}=720±50 K). Compositions

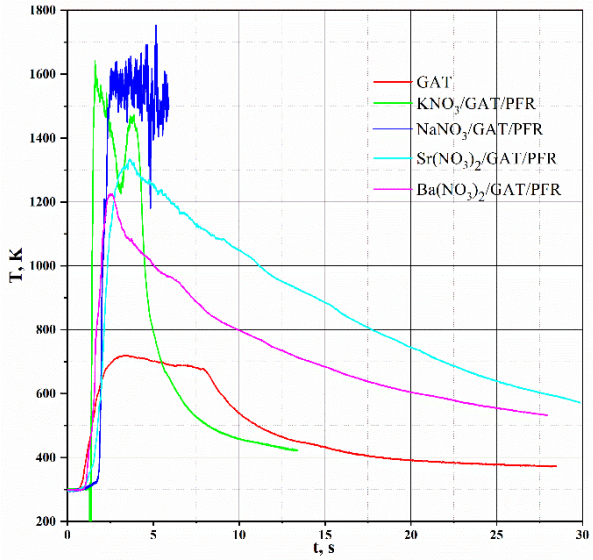

Figure 6. Combustion temperature of GAT and pyrotechnic compositions.

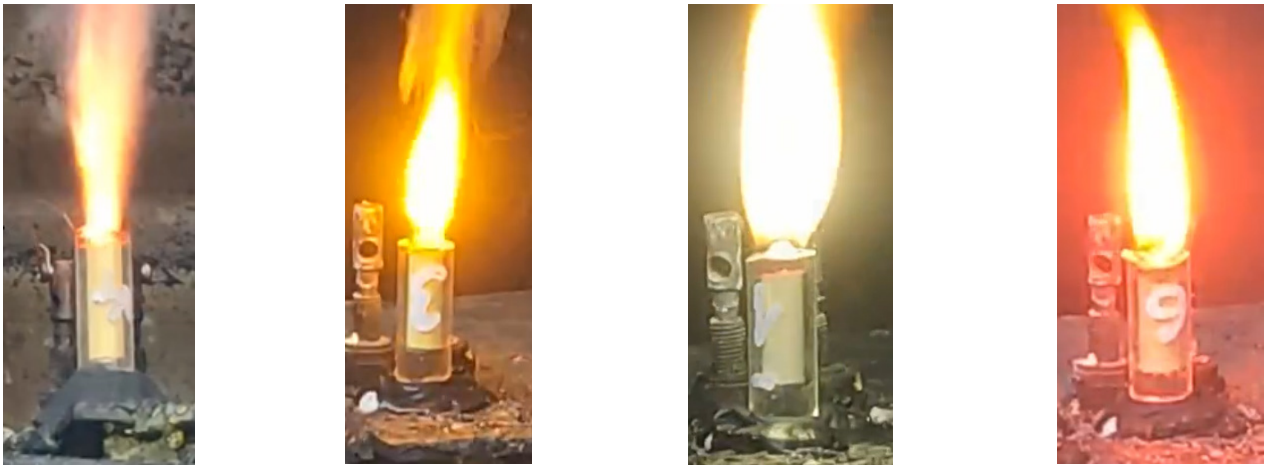

(a) (b) (c) (d)

Figure 5. Flame of pyrotechnic samples: (a) KNO3/GAT/PFR; (b) NaNO3/GAT/PFR; (c) Ba(NO3)2/GAT/PFR; and (d) Sr(NO3)2/GAT/PFR.

containing KNO_3 and $NaNO_3$ showed similar combustion temperatures (T_{max}=1640±50 K), whereas compositions with $Ba(NO_3)_2$ and $Sr(NO_3)_2$ exhibited combustion temperatures of approximately 1220±50 K and 1330±50 K, respectively.

3.4 Heat of Combustion and Specific Volume of Gaseous Products

The experimental results for the heat of combustion and specific volume of gaseous products in pyrotechnic compositions utilizing KNO_3, $NaNO_3$, $Ba(NO_3)_2$, and $Sr(NO_3)_2$ as oxidizers are presented in Fig. 7. When comparing theoretical calculations with experimental measurements, it is evident that the calculated heat of combustion and specific volume of gaseous products are lower than the experimental values. This discrepancy arises because the theoretical calculations performed using the COMBUS software assume isochoric (constant volume) conditions, which do not fully represent the actual combustion process within the bomb calorimeter. As the calorimeter cools to room temperature (~295 K), the thermodynamic equilibrium shifts from the conditions at combustion temperature (~1500 K). During cooling, phase transitions occur, such as the condensation of water vapor and other combustion products changing phase, altering the equilibrium state, and leading to deviations between theoretical predictions and experimental results. However, this discrepancy is generally not significant.

The experimentally determined heat of combustion for the KNO_3/GAT/PFR and $NaNO_3$/GAT/PFR compositions ranged from 741.97-973.24 kcal.kg^{-1} and 935.81-1139.13 kcal.kg^{-1}, respectively. In comparison, the $Ba(NO_3)_2$/GAT/PFR and $Sr(NO_3)_2$/GAT/PFR compositions exhibited lower values, ranging from 719.30-822.99 kcal.kg^{-1} and 779.95-920.22 kcal.kg^{-1}, respectively. The specific volume of gaseous products for the KNO_3/GAT/PFR and $NaNO_3$/GAT/PFR compositions ranged from 334.51-421.81 L.kg^{-1} and 380.46-432.87 L.kg^{-1}, respectively. In contrast, higher values were observed for the $Ba(NO_3)_2$/GAT/PFR and $Sr(NO_3)_2$/GAT/PFR compositions, ranging from 383.96-496.69 L.kg^{-1} and 413.34-567.41 L.kg^{-1}, respectively.

As the oxygen balance increases positively, the specific volume of gaseous products decreases across all pyrotechnic compositions. Conversely, the specific volume increases as Ω becomes more negative. This phenomenon is attributed to the higher GAT content in the compositions at lower Ω values. Since GAT is a highly gas-generating compound, increasing its concentration results in a greater specific volume of gaseous products. Among the studied compositions, the $Sr(NO_3)_2$/GAT/PFR system exhibits the highest gas-generation capacity, reaching a maximum specific volume of 567.41 L.kg^{-1} at a composition ratio of 60/30/10 (Ω = -24.93 %), as shown in Fig. 7(d). Similar trends are observed in other pyrotechnic systems, with heat of combustion increasing and specific

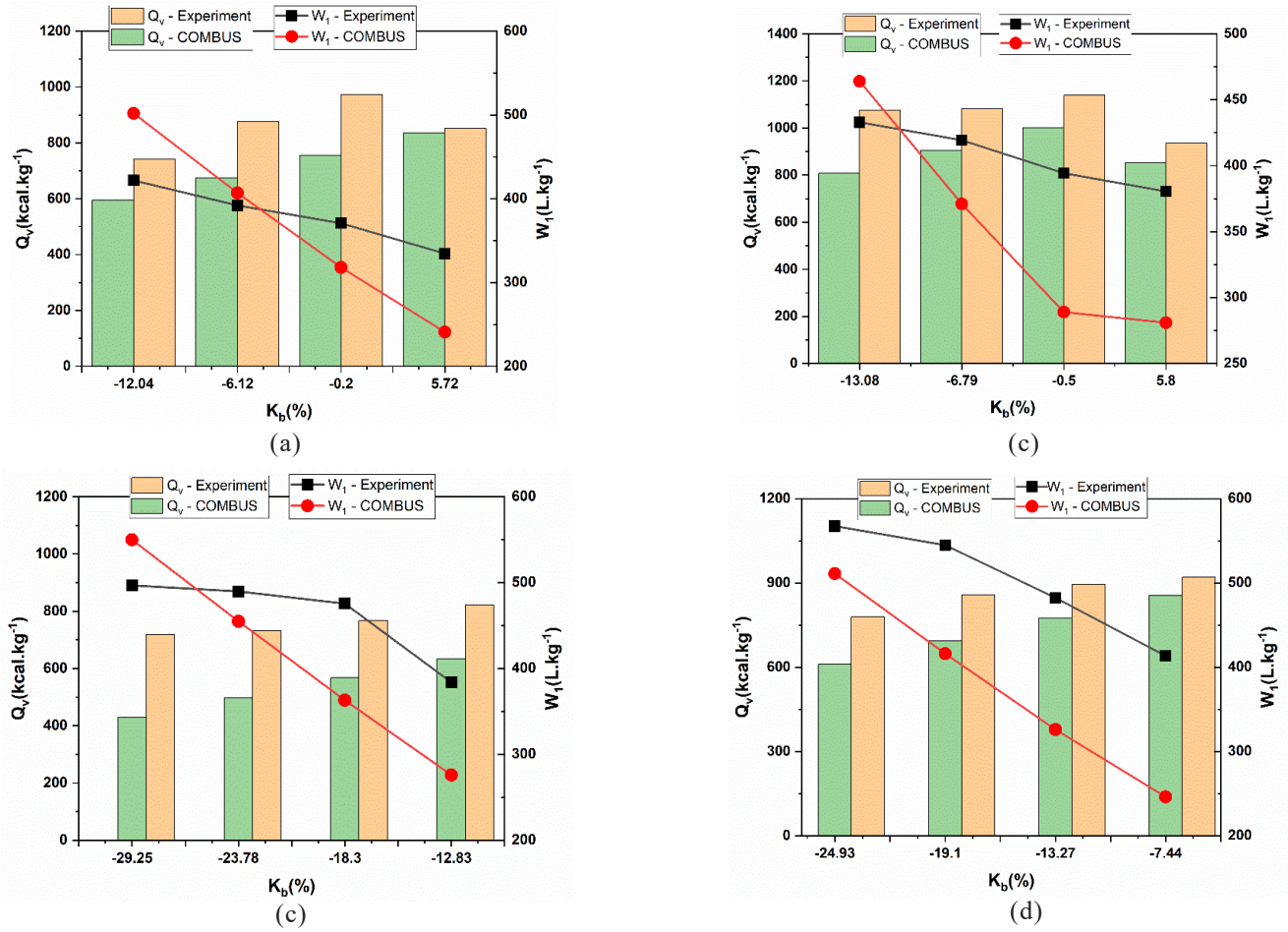

Figure 7. Effect of oxygen balance on the heat of combustion and specific volume of gaseous products: (a) KNO3/GAT/PFR; (b) NaNO3/GAT/PFR; (c) Ba(NO3)2/GAT/PFR, and (d) Sr(NO3)2/GAT/PFR.

Table 2. Ignition temperature of the pyrotechnic compositions

Oxidizer (%)	GAT (%)	PFR (%)	Ignition temperature T_i, K			
			$NaNO_3$	KNO_3	$Ba(NO_3)_2$	$Sr(NO_3)_2$
80	10	10	664.46			520.45
75	15	10	665.95			519.30
70	20	10	669.05	≥ 673	≥ 673	516.60
65	25	10	≥ 673			516.40
60	30	10	≥ 673			514.05

volume decreasing as Ω rises from negative values toward zero.

For the $NaNO_3$/GAT/PFR and KNO_3/GAT/PFR systems, the heat of combustion peaks near Ω = 0, aligning with theoretical calculations from COMBUS software and established thermodynamic principles. Likewise, the other two systems show a similar tendency for heat of combustion to approach maximum values as Ω approaches zero. Notably, the KNO_3/GAT/PFR composition at a 70/20/10 ratio demonstrates a relatively high burning rate of 4.48 $mm.s^{-1}$ while maintaining a considerable gas-generation capacity of 421.81 $L.kg^{-1}$.

3.5 Determination of Sensitivity of Pyrotechnic Compositions

The friction and impact sensitivity values were experimentally determined for GAT and the pyrotechnic compositions, with results exceeding 360 N for friction and 25 J for impact, respectively. These findings indicate that both GAT and the pyrotechnic compositions exhibit very low sensitivity to friction and impact. Thermal sensitivity was evaluated based on the ignition temperatures of the pyrotechnic compositions, as summarized in Table 2. The ignition temperatures of compositions containing KNO_3, $NaNO_3$, and $Ba(NO_3)_2$ were approximately 673 K or higher, whereas the $Sr(NO_3)_2$-based composition exhibits a lower ignition temperature of approximately 516 K.

Overall, these findings suggest that the tested compositions possess relatively high ignition temperatures, indicating low thermal sensitivity and thus good safety characteristics under thermal exposure.

4. CONCLUSION

GAT was used in low-exothermic, gas-generating pyrotechnics. Four GAT-based compositions (KNO_3/GAT/PFR, $NaNO_3$/GAT/PFR, $Ba(NO_3)_2$/GAT/PFR, $Sr(NO_3)_2$/GAT/PFR) containing 10 wt.% PFR were systematically studied. Sensitivity tests demonstrated the formulations' thermal stability and low mechanical sensitivity, indicating their suitability for practical applications.

A systematic formulation matrix was developed by varying oxidizer types in combination with the gas-generating compound GAT. Key energetic properties, including heat of combustion, burning rate, flame temperature, specific volume of gaseous products, and thermal decomposition behavior, were comprehensively evaluated using experimental methods.

Notably, the $Sr(NO_3)_2$/GAT/PFR composition at a ratio of 60/30/10 produces the highest specific gas volume of 567.41 $L.kg^{-1}$ alongside a relatively low heat of combustion of 779.95 $kcal.kg^{-1}$, outperforming other tested formulations. In comparison, the KNO_3/GAT/PFR formulation at 70/20/10 exhibits a respectable burning rate of 4.48 $mm.s^{-1}$, with a heat of combustion of 741.97 $kcal.kg^{-1}$ and a specific gas volume of 421.81 $L.kg^{-1}$. These results highlight the superior gas-generating capacity of the $Sr(NO_3)_2$-based formulation while confirming the practical potential of the KNO_3-based system. Together, these findings demonstrate the promise of GAT-based pyrotechnic formulations with PFR for enhanced performance and safety in gas-generating applications.

REFERENCES

1. Henry III GH, Solverson MS, inventors; Automotive Systems Laboratory Inc, assignee. Gas generating propellant. United States patent US 5,538,567. 1996 Jul. 23.
2. Máša V, Kuba P. Efficient use of compressed air for dry ice blasting. J Cleaner Prod. 2016;111, Part A:76-84. doi: 10.1016/j.jclepro.2015.07.053.
3. Qian Y, Han Z, Zhang Y, Du Z, Zhao Y, Yang Y, et al. Synthesis, Structure, and Energetic Properties of 1, 5-Diaminotetrazolium Sulfate Salts. J Heterocycl Chem. 2016;53(2):651-7. doi: 10.1002/jhet.2579.
4. Ambekar A, Kim M, Lee W-H, Yoh JJ. Characterization of display pyrotechnic propellants: Burning rate. Appl Therm Eng. 2017;121:761-7. doi: 10.1016/j.applthermaleng.2017.04.097.
5. Parate BA. Gas Generator Pyrotechnics Using Gun Propellant Technology Methods. International Journal of Aerospace and Mechanical Engineering. 2022;16(3):81-7.
6. Parate B. Thermodynamic aspects of solid propellant gas generator for aircraft application. Seatific Engineering Research Journal. 2023. doi: 10.14744/seatific.2023.0004.
7. Dixit VK, Deodhar KD, Parate BA. Qualification Testing, Evaluation and Test Methods of Gas Generator for IEDs Applications. Def Sci J. 2021;71(4):462-9. doi: 10.14429/dsj.71.16601.
8. Ebeling H, Schmid H, Eisenreich N, Weiser V. Development of gas generators for fire extinguishing. Propellants Explos Pyrotech. 1997;22(3):170-5. doi: 10.1002/prep.19970220314.
9. Schmid H, Eisenreich N, Baier A, Neutz J, Schröter D, Weiser V. Gas generator development for fire protection

purpose. Propellants Explos Pyrotech. 1999;24(3):144-8.
10. Parate BA, Sahu A, Shetty C, Shekhar H, Chandel S, Dixit V, et al. Experimental Investigation on burning behaviour of different Propellants in Closed Vessel of Gas generator Cartridge for water-jet application. 2019 International Conference on Range Technology (ICORT); 2019: IEEE.
11. Dimitrova Z, Maréchal F. Gasoline hybrid pneumatic engine for efficient vehicle powertrain hybridization. Appl Energy. 2015;151:168-77. doi: 10.1016/j.apenergy.2015.03.057.
12. Wang HS, Du ZM. Progress in synthesis and properties of nitrogen-rich compounds. Chin J Energ Mater. 2011;13(3):196-9.
13. Han Z, Yao Q, Du Z, Tang Z, Cong X, Zhao L. Single Crystal, Molecular Accumulation and Thermal Analysis of Tetrazolo [l, 5-b][1, 2, 4] triazine. J Heterocycl Chem. 2016;53(1):280-3. doi: 10.1002/jhet.2307.
14. Date S, Boonyarat P, Kazumi T. Screening test of gas-generating agents using closed strand burner. Journal of the Japan Explosives Society. 2002;63(4):209-15.
15. Dimitrova Z, Lourdais P, Maréchal F. Performance and economic optimization of an organic rankine cycle for a gasoline hybrid pneumatic powertrain. Energy. 2015;86:574-88. doi: 10.1016/j.energy.2015.04.047.
16. Talawar MB, Sivabalan R, Asthana SN, Singh H. Novel Ultrahigh-Energy Materials. Combust Explos Shock Waves. 2005;41(3):264-77. doi: 10.1007/s10573-005-0031-1.
17. Yu-Lin Peng C-WW, inventor; National Chung Shan Institute of Science and Technology, assignee. Preparation of guanidinium 5'5-azotetrazolate. United States patent US 5877300. 1999 Mar. 2.
18. Lenahan S, Salan J, Head I. Improvements in the Synthesis of Guanidinium Azotetrazolate (GUzT). NSWC IHD. 2007.
19. Cheng S-R, Cheng K-F, Liu M-H, Hong Y-S, Chen C. Computational study of decomposition mechanisms and thermodynamic properties of molecular-type cracking patterns for the highly energetic molecule GZT. J Mol Model. 2013;19:3705-17. doi: 10.1007/s00894-013-1903-z.
20. Steinhauser G, Klapötke TM. "Green" pyrotechnics: a chemists' challenge. Angew Chem, Int Ed 2008;47(18):3330-47. doi: 10.1002/anie.200704510.
21. An T, Zhao F-Q, Wang Q, Sheng D-L, Pan Q, Feng H, et al. Preparation, characterization and thermal decomposition mechanism of guanidinium azotetrazolate (GUZT). J Anal Appl Pyrolysis. 2013;104:405-11. doi: 10.1016/j.jaap.2013.06.005.
22. Hudson MK, Wright AM, Luchini C, Wynne PC, Rooke S. Guanidinium azo-tetrazolate (GAT) as a high performance hybrid rocket fuel additive. J Pyrotechnics. 2004;19:37-42.
23. Cao C, Zhang D, Lu S, Liu C. Thermal decomposition behavior, kinetics, thermal safety and burning characteristics of guanidinium-5-aminotetrazole (GA) based propellants. J Therm Anal Calorim. 2019;143(1):609-18. doi: 10.1007/s10973-019-09063-1.
24. Schmid H, Eisenreich N. Investigation of a Two-Stage Airbag Module with Azide-Free Gas Generators. Propellants Explos Pyrotech. 2000;25(5):230-5.
25. Abe M, Ogura T, Miyata Y, Okamoto K, Date S, Kohga M, et al. Evaluation of gas generating ability of some tetrazoles and copper (II) oxide mixtures through closed vessel test and theoretical calculation. Sci Tech Energetic Materials. 2008;69(6):183-9.
26. Siegfried Dr. Zeuner, Roland Dr. Schropp, Karl-Heinz Rödig, Reimann UD, inventors; ZF Airbag Germany GmbH, assignee. Process for the preparation of a gas generating composition. Germany patent DE 10230402B4. 2007.
27. Harikrishnan ES, Hariharanath B, Vineeth GM, Purushothaman P. Thermokinetic analysis and performance evaluation of guanidinium azotetrazolate based gas generating composition for testing of solid rocket motor nozzle closures. Propellants Explos Pyrotech. 2018;43(10):1006-12. doi: 10.1002/prep.201800103.
28. Harikrishnan ES, Hariharanath B, Vineeth GM, Nimesh S, Vikram T, Pal S. Development of a Cool Composite Propellant Based on Guanidinium Azotetrazolate for Air Heater Igniter Application. Propellants Explos Pyrotech. 2023;48(3):e202200190. doi: 10.1002/prep.202200190.
29. Han ZY, Yang YZ, Du ZM, Li ZY, Yao Q, Wang YH, et al. The formulation design and performance test of gas generators based on guanidinium azotetrazolate. Propellants Explos Pyrotech. 2017;42(3):276-83. doi: 10.1002/prep.201600164.
30. Hoang TH, Nguyen TT, Nguyen VD. Solubility determination and recrystallization studies of guanidinium 5,5'-azotetrazolate. Conference: New Trends in Research of Energetic Materials; 2023; Czech Republic.
31. STANAG4487. Explosive, friction sensitivity tests. NATO. 2009 Oct 29; 18.
32. GOST 4545-88. Explosives, high. Sensitivity characteristics determination for impact. USSR State Committee for Standards. 1988 Sept 19
33. Abràmoff MD, Magalhães PJ, Ram SJ. Image processing with ImageJ. Biophotonics Int. 2004;11(7):36-42.
34. Hosseini S, Eslami A. Thermoanalytical investigation of relative reactivity of some nitrate oxidants in tin-fueled pyrotechnic systems. J Therm Anal Calorim. 2010;101(3):1111-9. doi: 10.1007/s10973-010-0813-x.

CONTRIBUTORS

Dr Nguyen Duy Tuan obtained his PhD from the Mendeleev University of Chemical Technology of Russia and working as a Scientist at the Department of Energetic Materials of Le Quy Don Technical University, Vietnam. His research interests include: Pyrotechnics, propellant and rocket fuel.

In the current study, he formulated the study framework, carried out an extensive literature analysis, and designed the methodology.

Prof Dam Quang Sang obtained his PhD from the Mendeleev University of Chemical Technology of Russia and working as a Scientist at the Department of Energetic Materials of Le Quy Don Technical University, Vietnam. His research interests include: Calculation of explosion and combustion processes, the preparation of pyrotechnic mixtures and commercial explosives.
In the current study, he performed calculations and revised the manuscript.

Mr Mai Van Thanh is a Postgraduate student at Department of Energetic Materials of Le Quy Don Technical University. His research field is pyrotechnic compositions.
In this study, he conducted experimental measurements and analyzed the data.

Dr Hoang Trung Huu obtained his PhD from the Mendeleev University of Chemical Technology of Russia and working at the Department of Energetic Materials of Le Quy Don Technical University, Vietnam. His research area is the combustion of energetic materials and explosive technology.
In this research, he proposed the research idea, took responsibility for the results, and edited the manuscript.